

PCEST: Positive Contrast using Chemical Exchange Saturation Transfer

E. Vinogradov¹, T. C. Soesbe², J. A. Balschi³, D. A. Sherry^{2,4}, and R. E. Lenkinski¹

¹Department of Radiology, Beth Israel Deaconess Medical Center, Harvard Medical School, Boston, MA, United States, ²Advanced Imaging Research Center, University of Texas Southwestern Medical Center, Dallas, TX, United States, ³NMR Laboratory for Physiological Chemistry, Brigham and Women's Hospital, Harvard Medical School, Boston, MA, United States, ⁴Department of Chemistry, University of Texas at Dallas, Dallas, TX, United States

Introduction

A class of MRI contrast agents was introduced recently based on altering image contrast using the Chemical Exchange Saturation Transfer (CEST) mechanism. It is based on the selective presaturation of the small pool of exchanging protons and can be switched "on" and "off" using suitable RF irradiation¹. In PARACEST, exogenous complexes of PARAMagnetic lanthanides are used for CEST imaging^{2,3}. Potentially, PARACEST agents can be detected at very low concentrations and are also very sensitive to the agent environment. Here we will refer to small organic molecules as DIACEST agents, and use CEST to refer to the class of experiments in general. A standard CEST scheme creates negative contrast – i.e., it decreases the signal. Here we introduce the new scheme that creates a *positive* CEST contrast. The new scheme, dubbed *Positive CEST (PCEST)*, results in the increased signal in the presence of the agent. In addition, it leads to substantial background suppression. The sequence utilizes changes in apparent T_1 in the presence of the saturation of the bound pool⁴. It also has similarities with spin-lock experiments⁵. The sequence allows more efficient utilization of the dynamic range and can potentially avoid artifacts associated with the strong background signal. Here we will discuss the principles and characteristics of this new scheme and its application to the detection of the DIACEST and PARACEST agents.

Materials and Methods

The experiments were performed on the Varian Innova 400MHz vertical bore system, using a high resolution 5mm probe (for spectroscopy experiments) or custom-built coil (for imaging experiments). The sequence was tested for applicability with DIACEST and PARACEST agents, and representative agents from each group were tested. For DIACEST, 50mM solution of Creatine was used; and for PARACEST, 10mM solution of EuDOTA4AmC or solutions of EuDOTA4AmCE in various concentrations. In addition, a 4% agar phantom containing EuDOTA4AmCE agent was imaged.

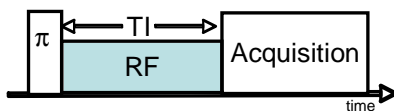


Figure 2. Schematic of the PCEST sequence: (i) inversion pulse, (ii) RF of length TI (optimized), (iii) image acquisition or spectroscopy.

Results and Discussion

The apparent longitudinal relaxation (R_{1app}) in the presence of saturating RF was measured as a function of the RF off resonance value, as well as a function of B_1 strength. R_{1app} as a function of off-resonance is shown in Fig.1 for DIACEST and PARACEST agents. As expected, when the RF is exactly on-resonance with the exchanging pool ("RF ON") the R_{1app} is increased. Overall, the R_{1app} vs offset agrees with the Z-spectra. The increase in apparent relaxation depends on the exchange parameters, as well as on the RF intensity. Preliminary data suggests that faster exchange rates require higher RF power to induce observable effects. Similar to CEST experiments, paramagnetic compounds may lead to bigger R_{1app} changes; however, higher RF power may be needed.

The increment in R_{1app} can be used to create the positive CEST contrast. The sequence schematic is shown in Fig.2. First, the length of the saturation pulse, TI, is selected such as to result in the signal null for "RF OFF", i.e. when the RF frequency is placed at the value symmetrical around water to "RF ON". The signal intensity as a function of B_1 was monitored for "RF ON" and "RF OFF" for a given TI. A representative result is shown in Fig. 3 for PARACEST. There is an optimal B_1 value for which the signal with "RF ON" is positive, while the signal with "RF OFF" is still close to null. This B_1 intensity is close to the optimal B_1 for the CEST experiments⁶, $B_1 \sim 1/\tau_b$, where τ_b is the lifetime of the exchanging pool. At the same time, R_{1app} increases with the increasing B_1 intensity (results not shown).

This principle can be combined with any imaging sequence to result in positive contrast CEST images (PCEST). Here, we have used a spin echo sequence for imaging. The PCEST images obtained for Creatine and EuDOTA4AmCE are shown in Fig.4.

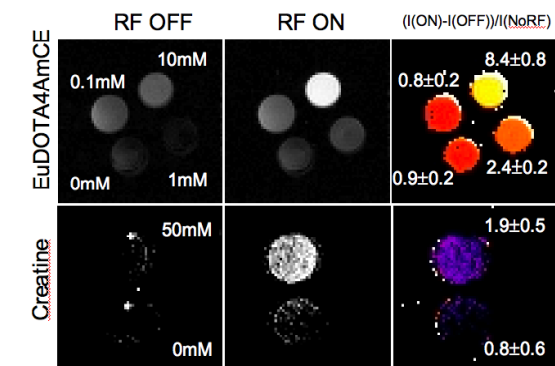


Figure 4. Positive CEST images acquired for PARACEST agent (top row) and DIACEST agent (bottom row). The right column displays normalized difference image (PCEST effect in %)

Ideally, the RF OFF image should be completely null, however, changes in T_1 and RF inhomogeneity resulted in the non-zero intensity of the images. The PCEST effect sizes are shown on the figure. Overall the effect sizes are lower than with the standard CEST sequences (confirmed by simulations, not shown). To check influence of the magnetization transfer from a semi-solid pool, the sequence was also successfully tested in the 4% agar with 10mM EuDOTA4AmCE agent. The only parameter that needs to be adjusted is TI (from 1.4s in water to 0.9s in agar).

Currently, the sequence is tested *in-vivo*. It is expected that the sequence will need to be tailored to account for the presence of multiple T_1 s.

Conclusions

Here we demonstrate the possibility of positive CEST contrast. The positive contrast has the advantages of better utilization of the dynamic range, suppression of the background signal, and potentially lower sensitivity to background artifacts. The disadvantages may include lower absolute contrast sizes and sensitivity to T_1 . Work is underway to further improve the sequence and to verify its applicability *in-vivo*.

References

1. Ward K, *et al.* *JMR* 2000;**143**:79; 2. Zhang S, *et al.* *JACS* 2001;**123**:1517;
3. Aime S, *et al.* *JACS* 2002;**124**:9364; 4. Baguet E, *et al.* *JMR A* 1994;**108**:189; 5. Santyr GE, *et al.* *MRM* 1994;**32**: 43; 6. Woessner DE, *et al.* *MRM* 2005;**53**:790

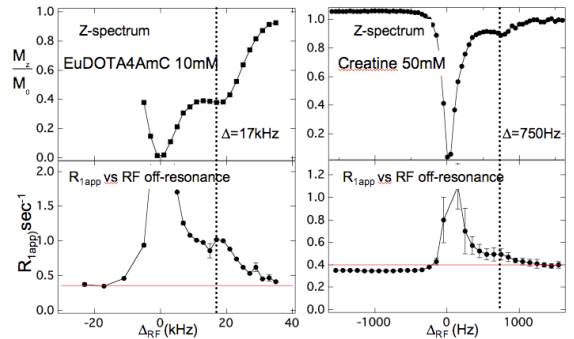


Figure 1. Z-spectra (top) and R_{1app} vs RF off-resonance (bottom) for 10mM EuDOTA4AmC (left) and 50mM Creatine (right).

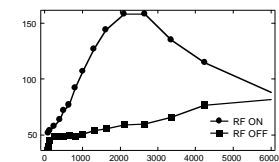


Figure 3. Signal intensity for "RF ON" and "RF OFF" as a function of B_1 for $T=2$ sec (adjusted for signal null with no RF).